iScience

CellPress
OPEN ACCESS

Article

Scramblase activity of proteorhodopsin confers physiological advantages to *Escherichia coli* in the absence of light

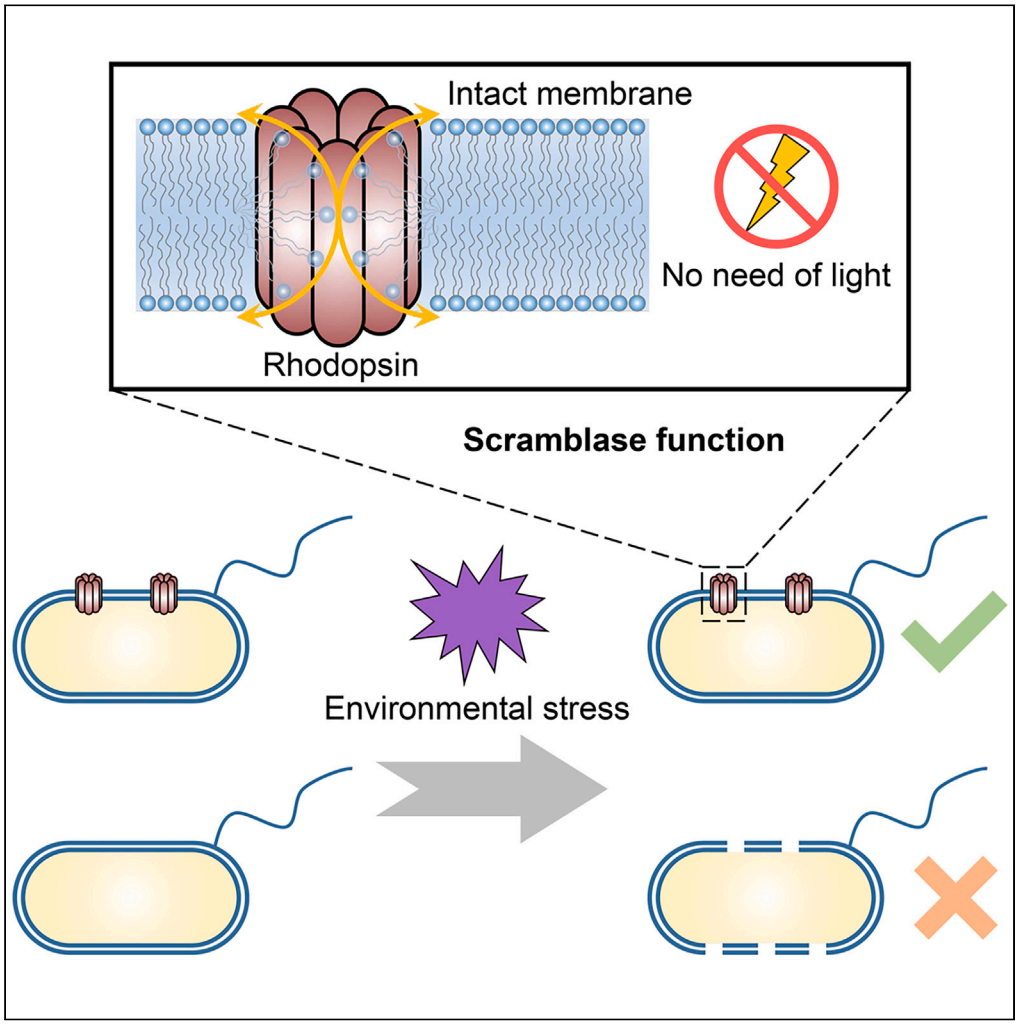

Jiayu Fang, Yanping Zhang, Taicheng Zhu, Yin Li

zhutc@im.ac.cn (T.Z.)
yli@im.ac.cn (Y.L.)

Highlights

ptqPR exhibited light-independent functions in addition to its light-dependent role

ptqPR could enhance the viability of *E. coli* under stress conditions without light

ptqPR increased tolerance by improving energy maintenance and membrane function

The non-canonical function of ptqPR was associated with its scramblase activity

Fang et al., iScience *26*, 108551
December 15, 2023
https://doi.org/10.1016/j.isci.2023.108551

iScience

CellPress
OPEN ACCESS

Article

Scramblase activity of proteorhodopsin confers physiological advantages to *Escherichia coli* in the absence of light

Jiayu Fang,[1,2] Yanping Zhang,[1] Taicheng Zhu,[1,*] and Yin Li[1,3,*]

SUMMARY

Microbial rhodopsins are widely distributed in the aqua-ecosystem due to their simple structure and multi-faceted functions. Conventionally, microbial rhodopsins are considered to be exclusively light active. Here, we report the discovery of light-independent function of a proteorhodopsin from a psychrophile *Psychroflexus torquis* (ptqPR). ptqPR could improve the growth and viability of *Escherichia coli* cells under stressful conditions in the absence of light, and this was achieved by improving the energy maintenance, membrane potential, membrane fluidity, and membrane integrity. We further show that this non-canonical function of PR is related to its scramblase activity. PR mutants which lost scramblase activities also lost their ability to confer physiological advantages in *E. coli*. These findings shed light on why microbial rhodopsins are widely distributed in ecological systems where light is inaccessible.

INTRODUCTION

Microbial rhodopsins (type I rhodopsins) are light-harvesting proteins that are widely distributed in bacteria, archaea, and even giant viruses.[1,2] The majority (>79%) of type I rhodopsins is from proteobacteria, designated as proteorhodopsin (PR).[3–5] Conventionally, rhodopsins are considered exclusively light active due to its functions of light-driven ion pumping, light sensing, and light-gated ion channeling.[6–10] A rhodopsin becomes light active through binding with retinal chromophore at the lysine residue which is located in its seventh transmembrane helix and conserved among most rhodopsins.[5] Rhodopsins lacking the conserved lysine residue (designated as Rh-noKs) are not light active unless introducing the lysine residue, demonstrating the importance of a complete structure of rhodopsins in maintaining its light-associated activity.[11]

Rhodopsin genes with retinal chromophore-binding site are usually discovered in the sunlight zone of the sea, which is approximately 200 m beneath the sea surface.[12] Interestingly, putative rhodopsin genes with retinal chromophore-binding site have also been identified in the organisms residing at 500–1000 m deep beneath the sea surface, where the sunlight can barely penetrate.[12] Conceivably, the rhodopsins in deep sea microbes would not exert light-associated activity as no light is available. This poses questions why rhodopsins are frequently found in deep sea microbes, whether rhodopsins play a light-independent function, and if so, what the function is.[12–15] Recently, Song et al. reported that a PR-expressing *E. coli* strain showed a marginally but significantly higher viability than that of the control strain under darkness in a 9-month survival experiment.[15] Using single-cell Raman spectroscopy, the authors further found that PR-expressing *E. coli* cells might have a higher lipid content, which is an indication of a more intact membrane. These observations provide experimental evidence supporting the hypothesis that PR might play a function in the absence of light. However, the exact function of PR under darkness remains unclear. Here, we show that overexpression of a PR from a psychrophile can enhance the viability of *E. coli* cells under stressful conditions. Moreover, we show PR can improve the energy maintenance and membrane biophysical properties of *E. coli*, including membrane potential, membrane fluidity, and membrane integrity. We further demonstrate that PR possesses scramblase activity and propose that the non-canonical function of microbial rhodopsin is related to this scramblase activity.

RESULTS

ptqPR showed light-driven proton-pumping activity when expressed in *E. coli*

Since PR represents the most abundant microbial rhodopsins compared to other types, a PR from a sea-ice psychrophile *Psychroflexus torquis* ATCC 700755,[16] designated as ptqPR, was chosen to study. The ptqPR was reported to function as a light proton pump and assumed to be responsible for the light-stimulated growth of *P. torquis*.[16] We expressed ptqPR in *E. coli* and confirmed its expression by western blot (Figure S1A). The membranes of the ptqPR-expressing *E. coli* strain exhibited a typical red color in the presence of retinal as reported in previous

[1]CAS Key Laboratory of Microbial Physiological and Metabolic Engineering, State Key Laboratory of Microbial Resources, Institute of Microbiology, Chinese Academy of Sciences, Beijing 100101, China
[2]University of Chinese Academy of Sciences, Beijing 100049, China
[3]Lead contact
*Correspondence: zhutc@im.ac.cn (T.Z.), yli@im.ac.cn (Y.L.)
https://doi.org/10.1016/j.isci.2023.108551

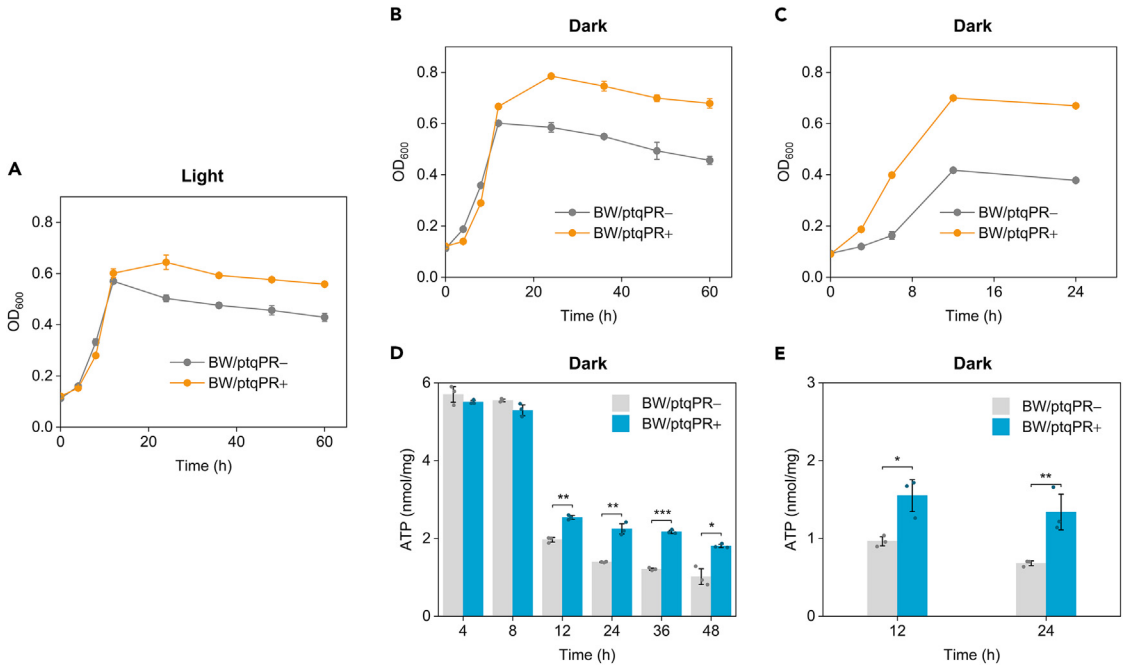

Figure 1. *E. coli* BW25113 strain harboring ptqPR shows improved growth and higher intracellular ATP level in the absence of light and retinal

(A–C) Strains BW/ptqPR$^+$ and BW/ptqPR$^-$ were cultured in M9+glucose medium. Growth profile under different conditions: (A) light, 10 μM retinal; (B) dark, no retinal; (C) dark, 30 μM CCCP.

(D and E) Intracellular ATP content of cells collected from the growth experiments shown in B and C, respectively. The data are presented as mean values and standard deviations of three replicates. *p < 0.05, **p < 0.01 and ***p < 0.001.

studies[17–20] (Figure S1B). The absorption spectrum of the membrane fraction of the ptqPR-expressing *E. coli* strain showed a clear absorbance at around 540 nm (Figure S1C). GFP-fusion expression of ptqPR showed that ptqPR proteins were mainly located on the cell membrane with no inclusion bodies formed (Figure S1D). In addition, the light-driven proton-pumping activity of ptqPR was confirmed by pH decrease upon illumination (Figure S1E).

ptqPR overexpression enhanced the growth and ATP levels of *E. coli* cells under stressful conditions in the absence of light

Growth experiments of ptqPR-expressing *E. coli* strain with or without retinal showed no difference when grown in glucose minimal medium under semi-aerobic conditions with illumination, suggesting that light did not stimulate the growth of PR-expressing *E. coli*. This is consistent with several previous studies,[21–24] and could be ascribed to the low light energy conversion rates of PRs[25] (Figure S2). Surprisingly, the ptqPR-expressing strain (BW/ptqPR$^+$) exhibited significantly higher OD_{600} value than that of the control strain harboring the empty vector (BW/ptqPR$^-$) upon entering the late logarithmic phase (after 12 h), and this beneficial effect was irrespective of the presence of light and retinal (Figures 1A and 1B). Concomitantly, the intracellular ATP levels of BW/ptqPR$^+$ cells grown to late logarithmic and stationary phase were significantly higher than that of BW/ptqPR$^-$ cells under darkness (Figure 1D). In addition, a flow cytometry analysis using Syto9/PI staining showed that BW/ptqPR$^+$ cells also possess higher viability (Figure S3).

Carbonyl cyanide 3-chlorophenylhydrazone (CCCP) is a proton motive force (PMF) uncoupler which can lead to collapse of PMF.[19] Addition of CCCP to the culture medium led to a 14.7% reduction in growth of BW/ptqPR$^+$ cells but a 35.3% reduction in the growth of BW/ptqPR$^-$ cells at 24 h in the absence of light and retinal (Figure 1C). Consistently, the intracellular ATP level of BW/ptqPR$^+$ cells was higher than that of BW/ptqPR$^-$ cells in the presence of CCCP (Figure 1E). The higher ATP levels of BW/ptqPR$^+$ cells in the presence and absence of CCCP indicate that PMF can be better maintained in BW/ptqPR$^+$ cells in the absence of light and retinal.

Moreover, since weak acids can also act as PMF uncoupler and thus affect the viability of microbial cells,[26] we examined the effect of weak acids treatment on the survival of BW/ptqPR$^+$ and BW/ptqPR$^-$ cells in the absence of light and retinal. As expected, BW/ptqPR$^+$ cells maintained considerably higher viability (Figures 2A and S4), and the intracellular ATP levels of BW/ptqPR$^+$ cells were higher than that of BW/ptqPR$^-$ cells during the treatment (Figure 2B). This further confirmed that PMF can be better maintained in ptqPR-expressing cells in the absence of light. Coincidently, the physiologically beneficial effects of ptqPR in the absence of light, which include improved cell growth, enhanced cell viability, and increased intracellular ATP levels, are exactly the same as those observed or expected from the conventional light-driven proton-pumping function of PR.[27–30]

In order to rule out the possibility that the observed beneficial effects of ptqPR were related to its conventional light-dependent activity, we inactivated the active sites of ptqPR responsible for proton translocation during light-dependent pumping.[6,31] Sequence alignment inferred

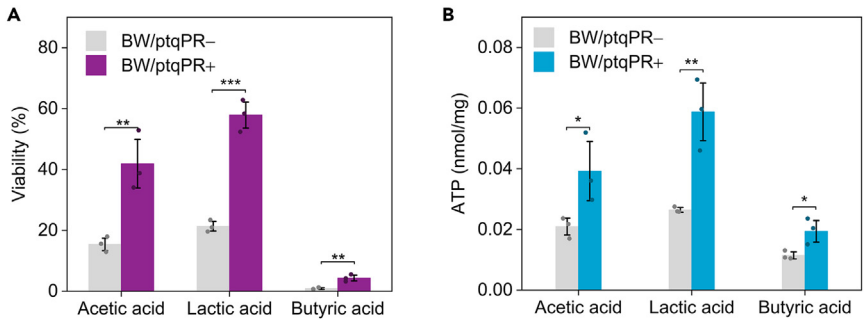

Figure 2. *E. coli* BW25113 cells harboring ptqPR cultured in the absence of light show higher viability and intracellular ATP levels upon weak acids treatment

(A and B) BW/ptqPR$^-$ and BW/ptqPR$^+$ cells were grown in the absence of light and retinal. Weak acids (5 g/L acetic acid, 5 g/L lactic, acid and 5 g/L butyric acid, respectively) were added to the cultures when cells grown to late logarithmic phase, treated for 3 h under dark condition. The culture collected was divided into two parts, one for determining viability (A) and the other for determining intracellular ATP levels (B). The data are presented as mean values and standard deviations of three replicates. *$p < 0.05$, **$p < 0.01$ and ***$p < 0.001$.

that Asp88 is the Schiff base counterion (proton acceptor) while Glu99 is the proton donor of ptqPR (Figures 3A and S5). Two single amino acid mutants of ptqPR, D88N and E99Q, completely abolished its light-driven proton-pumping activity (Figure 3B). Nevertheless, both mutants retained their ability to stimulate cell growth at the same level as the wild-type ptqPR in the absence of light (Figure 3C). We thus conclude that the physiologically beneficial effects conferred by ptqPR were not due to its conventional light-driven proton-pumping activity, but a yet unidentified light-independent mechanism.

ptqPR improved the membrane potential, membrane fluidity, and membrane integrity of *E. coli*

To better understand the mechanism underlying the non-canonical function of ptqPR, we compared the transcriptomes of BW/ptqPR$^+$ and BW/ptqPR$^-$ cells. The GO term and KEGG pathway enrichment analysis did not reveal significant differences in major metabolic pathways (Figure S6). However, the transcription levels of several cold shock proteins and phage shock proteins in BW/ptqPR$^+$ cells decreased significantly (Table S1). Low temperature and phage infection can cause stresses that often affect membrane structure.[33–36] Moreover, it was reported that phage shock proteins participate in a variety of membrane functions, including maintaining membrane integrity and PMF.[33,34] As such, we hypothesized that ptqPR might play membrane-protective functions, i.e., the expression of ptqPR might replace or compensate the role of environment-shock protein genes, leading to their reduced transcription.

To examine the hypothesis, we compared the membrane biophysical parameters of BW/ptqPR$^+$ and BW/ptqPR$^-$ cells, including membrane potential, membrane fluidity, and membrane permeability. The anionic dye $DiBAC_4(3)$ was used to analyze the bacterial cell membrane potential.[37] For cells with low membrane potential, the negatively charged dye can penetrate more easily, thus increasing the intensity of fluorescence, and vice versa (Note S1). The results showed that the fluorescence intensity of BW/ptqPR$^+$ cells was 15.7% lower than that of BW/ptqPR$^-$ cells, indicating a higher membrane potential and a higher PMF in BW/ptqPR$^+$ cells (Figure 4A). We then assessed the membrane fluidity using a fluorescent probe 1,6-diphenyl-1,3,5-hexatriene as described in literature[38] (Note S2). Comparing to BW/ptqPR$^-$ cells, BW/ptqPR$^+$ cells showed a 36.1% lower fluorescence polarization value, indicating that they possess a more fluid membrane (Figure 4B). Moreover, membrane permeability was assessed by measuring the leakage of intracellular electrolytes via electrical conductivity assay[39] (Note S3). BW/ptqPR$^+$ cell suspensions exhibited a 44.2% lower relative conductivity than that of BW/ptqPR$^-$ cell suspensions after 6 h, suggesting that BW/ptqPR$^+$ cells are able to maintain much higher cell integrity. Even after being treated with the detergent Triton, BW/ptqPR$^+$ still exhibited lower relative conductivity than that of the untreated BW/ptqPR$^-$ cells (Figure 4C). Taken together, these evidences suggest that the ptqPR is able to enhance the membrane potential, membrane fluidity, and membrane integrity of *E. coli* cells in the absence of light and retinal.

Scramblase activity of ptqPR may contribute to the light-independent function of ptqPR

The positive role of ptqPR in enhancing the membrane potential and membrane fluidity while reducing membrane permeability suggests that the membrane-expressed ptqPR affects the structure and function of membrane. In recent years, studies have revealed that a bacteriorhodopsin from the archaeon *Halobacterium salinarum* and bovine opsin show phospholipid scramblase activity.[40–42] While the physiological implications of scramblase are not yet known, a recent report studying the model scramblase TMEM16F suggests that it might help restore damaged cell membrane by increasing membrane fluidity and plasticity.[43] These studies prompted us to speculate about a possible link between the light-independent functions of ptqPR and scramblase activity.

To determine whether ptqPR possesses the phospholipid scramblase activity, we performed *in vitro* experiment using proteoliposomes. The use of proteoliposome,[44] which is consisted of purified ptqPR protein and artificial lipids, bypasses the complex interaction between ptqPR and cells, thus providing direct insight into the basic mechanism of ptqPR-membrane interactions. A fluorescent reporter lipid

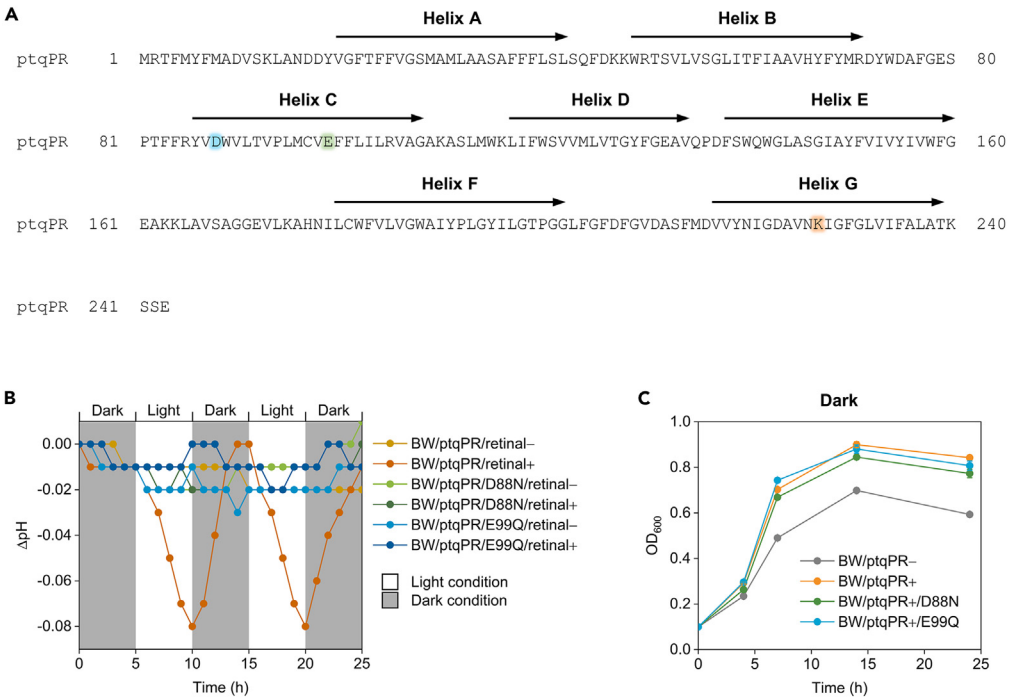

Figure 3. The physiological advantages conferred by ptqPR is not due to its conventional light-driven proton-pumping activity

(A) Bioinformatics analysis of the sequence of ptqPR. Membrane topology was predicted by TMHMM[32] (Figure S5A). The black arrow represents transmembrane helix. Alignment with other rhodopsin sequences (Figure S5B) revealed that Asp88, Glu99, and Lys227 could be the proton acceptor, the proton donor, and the retinal-binding site, respectively. Proton transport sites were mutated to their corresponding amide (D88N and E99Q).

(B) Proton pumping activity assay of ptqPR and its mutants. Light-induced proton fluxes were determined by pH changes in cell suspension. pH was normalized by the difference relative to the initial value. Gray area represents darkness and white area represents illumination.

(C) Growth profile of strains harboring ptqPR or its mutants in the absence of light and retinal.

1,2-dipalmitoyl-*sn*-glycero-3-phosphoethanolamine-*N*-(7-nitro-2,3-benzoxadiazol-4-yl) (NBD-PE) was applied to determine the scramblase activity as described in previous reports[40–42] (Note S4). The results showed that the loss of NBD fluorescence was approximately 50% for liposomes, but was 81.5% for proteoliposomes after dithionite treatment (Figure 5B). These indicated that ptqPR was able to scramble lipids from the inner to outer leaflet, thus confirming that ptqPR possesses phospholipid scramblase activity. To our knowledge, this is the first study reporting the scramblase activity of a proteorhodopsin, the most abundant microbial rhodopsins. Although the archaeal bacteriorhodopsin and mammalian rhodopsin (opsin)[41,42] have been reported to possess scramblase activity, two rhodopsins from the heliorhodopsin family did not exhibit it.[45] Therefore, further research is needed to assess the generality of scramblase activity among microbial rhodopsins.

To further investigate whether the non-canonical function of ptqPR is correlated with its phospholipid scramblase activity, we generated a series of ptqPR variants with decreased or abolished scramblase activity. This was achieved by mutating the polar amino acid residues into nonpolar ones according to the study reported by Verchère et al.[42] Four ptqPR variants (A, B, C, and D) were thus generated by mutating the polar amino acids in each group into alanine (Figure 6A). *E. coli* strains each harboring one of the four ptqPR variants exhibited significantly lower cell growth and intracellular ATP levels than that of BW/ptqPR^{+} strain and even BW/ptqPR^{-} strain, possibly due to a protein burden (Figures 6B and 6C). Next, we determined the phospholipid scramblase activity of mutant D (G143A-G147A-Y150A-Y155A), which showed the least growth. Significant decreased scramblase activity of mutant D was observed (Figures 6D and S7). The targeted mutation experiment showed that substitution of alanines for polar amino acid residues remarkably reduced the phospholipid scramblase activity of ptqPR and concomitantly led to the loss of its physiologically beneficial effects on *E. coli* (Figures 6B and 6C). Therefore, we infer that the phospholipid scramblase activity of ptqPR contributes to non-canonical function of ptqPR, conferring physiological advantages to the host cells in the absence of light.

To further validate our assumptions, we overexpressed two microbial rhodopsins that have been previously studied for their scramblase activity: a bacteriorhodopsin (BR) from *Halobacterium salinarum* and a heliorhodopsin (HeR) from *Thermoplasmatales archaeon*. The former has been reported to exhibit scramblase activity,[42] while the latter has not.[45] Unfortunately, the BR showed poor expression levels in *E. coli*, as evidenced by the limited color change upon incubation with retinal (Figure S9A), which aligns well with previous research.[47] In contrast, the HeR demonstrated significant expression in *E. coli*, exceeding even that of ptqPR (Figure S9B). However, the overexpression of HeR did not confer any growth advantages compared to the control group (Figure S9C). Acid treatment tests further revealed that HeR overexpression even led to decreased cell viability compared to strains with an empty vector (Figure S9D). This observation is consistent with findings from our

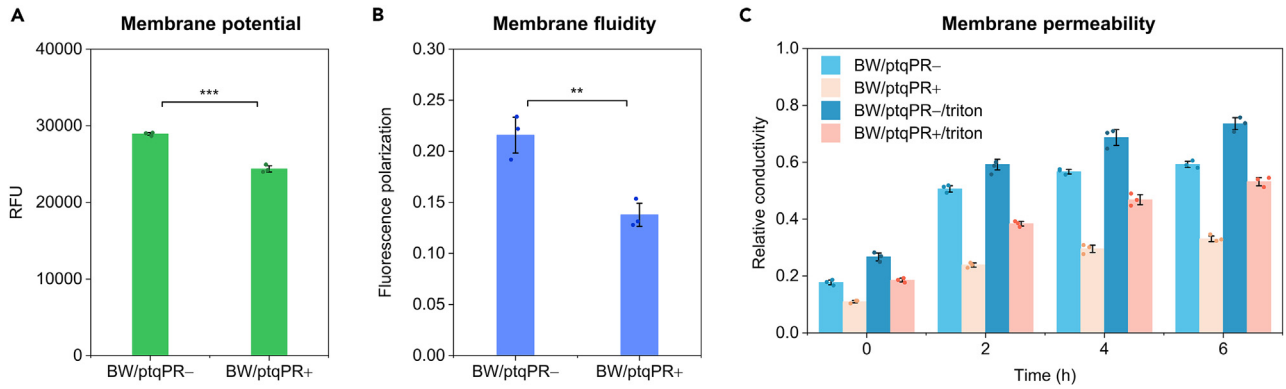

Figure 4. Membrane potential, membrane fluidity, and membrane permeability of *E. coli* BW25113 strain with or without ptqPR

(A) Strains were cultured in M9+glucose medium in the absence of light and retinal. When grown to stationary phase, cells were stained with $DiBAC_4(3)$ to measure fluorescence for membrane potential determination.

(B) Strains were cultured in M9+glucose medium in the absence of light and retinal. When grown to stationary phase, cells were stained with DPH to calculate fluorescence polarization for membrane fluidity determination.

(C) Strains were cultured in LB medium overnight in the absence of light and retinal. Then cells were collected and resuspended in 5% glucose solution. The electrolyte leakage in cell suspension was measured to determine membrane permeability. The data are presented as mean values and standard deviations of three replicates. $^{**}p < 0.01$ and $^{***}p < 0.001$.

site mutation of PR and lends support to our hypothesis that the phospholipid scramblase activity of ptqPR contributes to its non-canonical functions, providing physiological advantages to host cells even in the absence of light.

DISCUSSION

Although the light activities of microbial rhodopsins are well established, recent evidence indicates possible non-light functions.[48] For instance, deep-sea rhodopsins often lack light-related activity or retinal-binding capabilities compared to typical rhodopsins.[12] It seems that during evolution in oligotrophic and dark conditions, marine microbes tend to lose the chromophore (retinal) of rhodopsin along with its light-associated activity, but still retain the transmembrane peptide. Furthermore, over 10% of identified microbial rhodopsins, including the recently discovered group of HeRs, lack the conserved retinal-binding lysine residue (known as Rh-noKs).[11] These findings raise the possibility that microbial rhodopsins could also perform certain physiological functions in the absence of light, as speculated by previous studies.[12,13,48] However, definitive evidence supporting light-independent functions remains scarce.

In this study, we serendipitously discovered that *E. coli* cells harboring ptqPR could grow to a higher cell density when entering the late logarithmic phase without illumination. Furthermore, the ptqPR-expressing strain displayed a remarkable increase in viability toward treatment of weak acids, including acetic acid, lactic acid, and butyric acid. More importantly, we found that ptqPR-containing cells maintained a higher intracellular ATP level and a higher PMF under such conditions. Together, we conclude that PR can confer *E. coli* resistance to stressful environmental conditions such as nutrient limitation and weak acid stress in the absence of light.

Following the characterization of the physiological beneficial effects of ptqPR in the absence of light, the question of its underlying mechanism arises. We postulated that the membrane-expressed ptqPR may play a role in maintaining membrane integrity based on comparative transcriptome analysis that showed downregulation of phage shock protein and cold shock protein. To verify this hypothesis, we determined the biophysical parameters of the plasma membrane including membrane potential, membrane fluidity, and membrane permeability. Indeed, we observed improved biophysical characteristics of the membrane containing ptqPR. Using single-cell Raman spectroscopy, Song et al. discovered that non-PR cells displayed a decline in the Raman signal specific for unsaturated lipids when compared to PR cells, indicating that PR cells have a higher lipid content.[15] They speculated that PR might contribute to the stabilization of cytoplasmic membrane, which would help to maintain DNA and RNA levels and therefore cell viability.[15] While this hypothesis may be true especially under the test conditions applied by the authors, it largely ignored the role that maintenance energy plays during this process. To date, there is accumulating evidence showing that PMF and ATP play crucial roles in survival and stress tolerance of the microbes.[49–52] We therefore infer that the PR can enhance cell membrane integrity and fluidity, which helps to maintain a higher PMF for ATP synthesis, eventually leading to increased survival and stress tolerance in microbes.

In recent years, a few studies have reported that some of the rhodopsins have phospholipid scramblase activity, which is similar to recently described G protein-coupled receptor and TMEM16 (transmembrane protein 16) scramblase families.[41,53–55] Phospholipid translocation across the cellular membrane is facilitated by a series of ATP-dependent translocases (flippases/floppases) like P4-ATPases, ABC transporters, and ATP-independent scramblases.[56–58] The rate of phospholipid translocation mediated by scramblase (>10,000 s^{-1}) is faster than that by flippase/floppase (~100 s^{-1}).[53,59–61] Recently, a study of the model scramblase TMEM16F suggested that it could help repair the plasma membrane.[43] We therefore speculate that the scramblase activity of ptqPR might be a potential mechanism accounting for

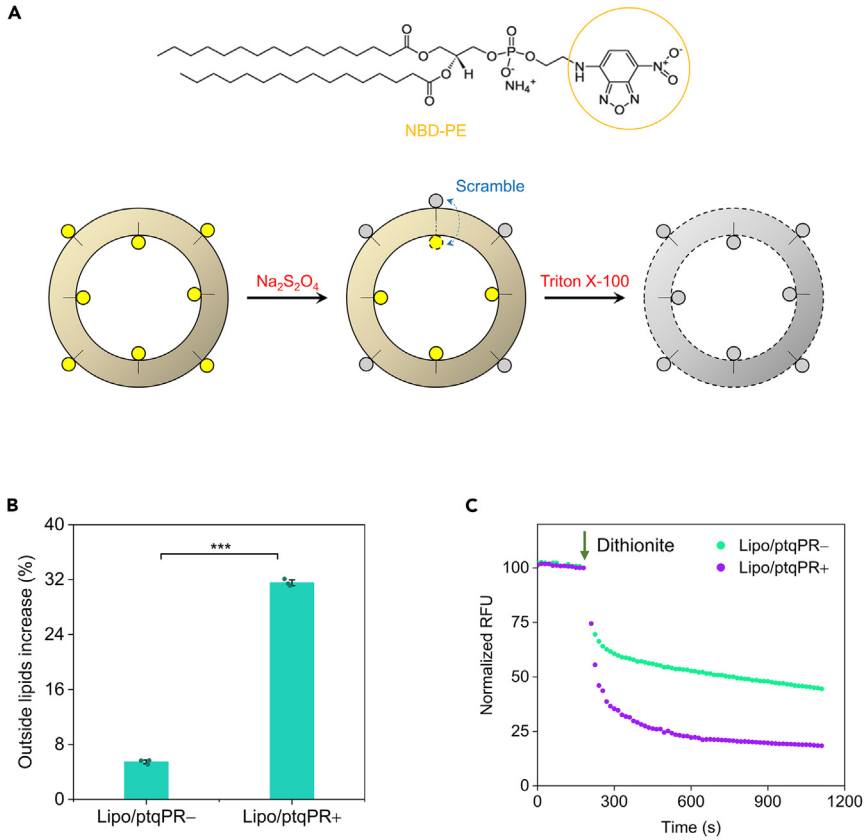

Figure 5. Determination of scramblase activity of ptqPR by *in vitro* assay

(A) Schematic diagram of the scramblase activity assay. Dithionite addition leads to a 50% decrease in fluorescence for cells or liposomes without phospholipid scrambling. Scramblase activity was characterized by outside lipids increase.

(B) Purified ptqPR proteins were reconstituted into NBD-labeled liposomes, the scramblase activity was then determined.

(C) Time courses of fluorescence loss from the scramblase assay in (B). The data are presented as mean values and standard deviations of three replicates. ***$p < 0.001$.

the improved membrane properties in *E. coli* cells. To explore the possible link between scramblase activity and the light-independent functions of ptqPR, we adopted a strategy involving substitution of alanines for polar amino acid residues and inactivated its phospholipid scramblase activity. As expected, the mutant was not able to confer physiologically beneficial effects to *E. coli* cells in terms of growth and ATP content. We also extended the investigation to other naturally occurring rhodopsins. Our findings revealed that overexpression of a HeR, which is reported to lack scramblase activity, similarly failed to improve cell growth and acid tolerance. These results further corroborate the link between scramblase activity and light-independent functions in rhodopsins. Future studies should explore whether other rhodopsins with scramblase activity also possess light-independent functions. For rhodopsins such as bacteriorhodopsin, which exhibit poor expression in *E. coli*, investigations may need to be conducted in their native hosts. Additionally, the oligomeric state of microbial rhodopsins has been known to influence their light-related activities.[42,62–64] While the impact of the oligomeric state on light-independent activities of rhodopsins warrants further investigation in future studies, it is evident that the mutation of ptqPR does not cause a significant change in its oligomeric state (Figure S10, Note S6). The findings provide evidence that phospholipid scramblase activity of ptqPR contributes to the non-canonical function of the protein.

In nature, nearly half of the microbial genomes in marine and terrestrial samples have rhodopsin-based light-harvesting systems, which is more than three times greater than reaction center-based photosystems (including oxygenic and anoxygenic photosystem).[65] It was believed that their widespread distribution was due to their simple structure and low energy requirements for the synthesis, which facilitated their spread via lateral gene transfer. However, rhodopsin systems are less efficient, at least one order of magnitude, than reaction center-based photosystems in terms of energy generation. Therefore, it can barely provide the energy required for cellular maintenance unless the light intensity and the number of copies per cell are very high.[3,25] In this connection, the ease and low cost of rhodopsin synthesis may not be able to entirely explain their current predominance in ecosystems.[25] If, however, rhodopsin also possesses light-independent functions, such as providing stress tolerance to aquatic bacteria as it does to the model organism *E. coli* shown in this work, this would further explain their enormous evolutionary competitive advantage over other photosystems.

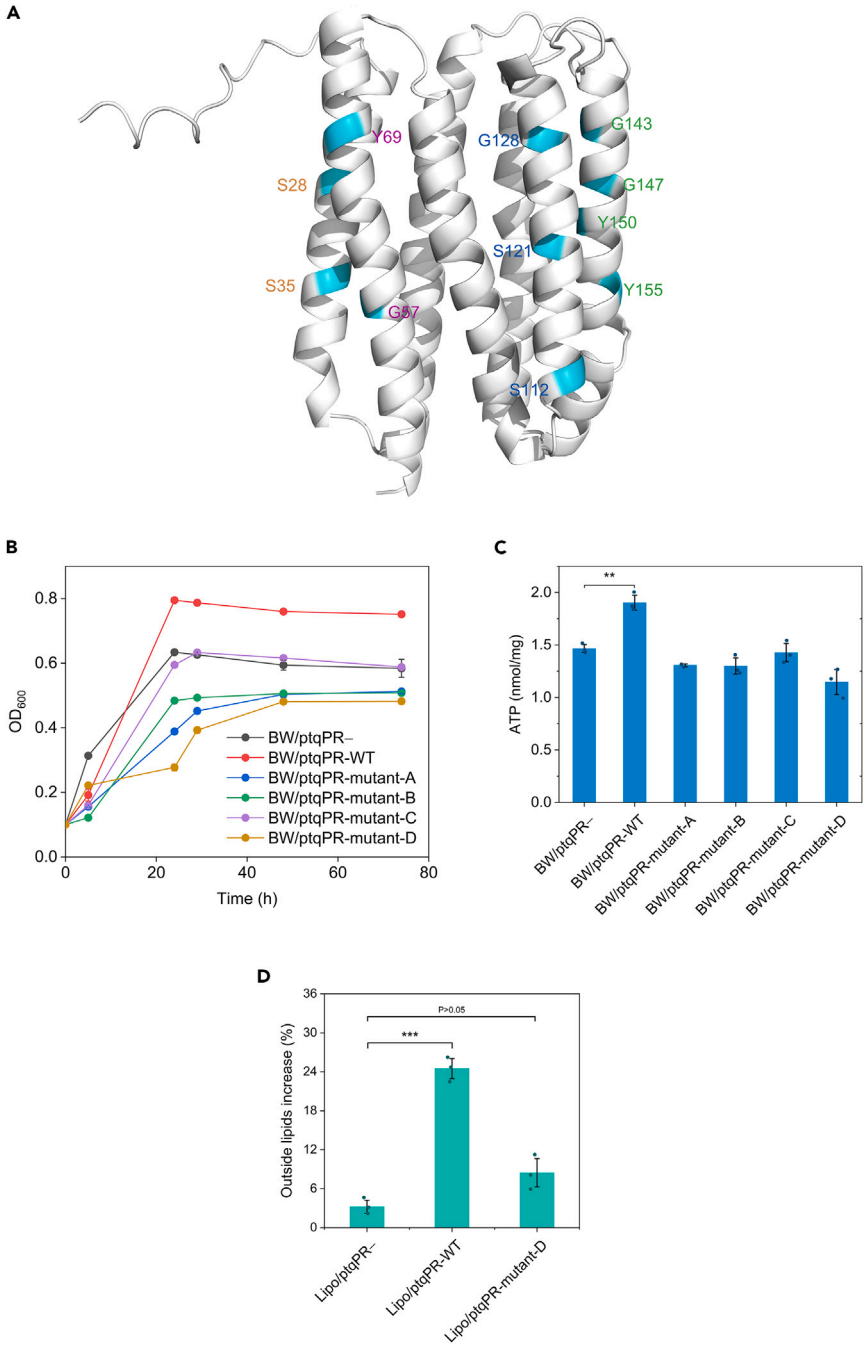

Figure 6. Inactivation of phospholipid scramblase of ptqPR abolished its physiological advantages in the absence of light and retinal

Based on structure alignment (Figure S8) of ptqPR (predicted by AlphaFold[46]) and bacteriorhodopsin (BR) (PDB ID: 4MD2), four groups (mutant A–D) of different polar amino acid residues, which may form potential lipid translocation pathway, were mutated to the non-polar amino acid alanine.

(A) Diagram of the predicted structure (made by PyMOL v.2.0) of ptqPR with labeled polar amino acids as possible phospholipid translocation cleft (Orange: mutant A; Purple: mutant B; Blue: mutant C; Green: mutant D).

(B and C) Determination of growth and intracellular ATP level of *E. coli* BW25113 strain harboring wild-type and mutant ptqPR.

(D) Determination of phospholipid scramblase activity of wild-type and mutant ptqPR (time courses of fluorescence loss are shown in Figure S7). The data are presented as mean values and standard deviations of three replicates. **p < 0.01 and ***p < 0.001.

Despite the widespread belief that microbial rhodopsins are exclusively light reactive, recent ecological, phylogenetic, and physiological investigations indicate that they may potentially function independently of light.[12–15,40,66] In this study, we demonstrate that a microbial rhodopsin can protect *E. coli* cells against environmental stresses in the absence of light. This hidden physiological role of rhodopsins may have been overlooked due to the past focus on their light-driven functions. If the same mechanisms are valid for marine bacteria *in situ*, the physiological and ecological implications of these ubiquitous proteins may need to be reevaluated from a new perspective in the future. Furthermore, this study may provide a mechanistic rationale for utilizing microbial rhodopsin as a device for biotechnology purposes such as improving the tolerance and robustness of microbial cell factories for biomanufacturing, as most of the fermentations are carried out in the absence of light.

Limitations of the study

We were unsuccessful in overexpressing the bacteriorhodopsin (with scramblase activity) in *E. coli* for our further validation of the relevance between the non-canonical function of microbial rhodopsin and its phospholipid scramblase activity.

STAR★METHODS

Detailed methods are provided in the online version of this paper and include the following:

- KEY RESOURCES TABLE
- RESOURCE AVAILABILITY
  - Lead contact
  - Materials availability
  - Data and code availability
- EXPERIMENTAL MODEL AND STUDY PARTICIPANT DETAILS
  - Bacterial strains
- METHOD DETAILS
  - Plasmids, bacterial strains and growth conditions
  - ATP measurement
  - Light-driven proton-pumping assay
  - Transcriptome analysis
  - Determination of membrane potential
  - Determination of membrane fluidity
  - Determination of membrane permeability
  - Protein purification
  - Preparation of small unilamellar vesicles and proteoliposomes
  - Scramblase activity assay
- QUANTIFICATION AND STATISTICAL ANALYSIS

SUPPLEMENTAL INFORMATION

Supplemental information can be found online at https://doi.org/10.1016/j.isci.2023.108551.

ACKNOWLEDGMENTS

This work was supported by the National Key R&D Program of China (2018YFA0901400 and 2021YFC2103500), the National Natural Science Foundation of China (31970039 and 32270058), and the Strategic Priority Research Program of the Chinese Academy of Sciences (XDB0480000). We thank Junjie Hu and Jie Ren (Institute of Biophysics, Chinese Academy of Sciences) for help in proteoliposome preparation. We thank Lei Su (Institute of Microbiology, Chinese Academy of Sciences) for help in confocal microscopy imaging and analysis. We thank Tong Zhao (Institute of Microbiology, Chinese Academy of Sciences) for technical support in flow cytometry analysis and Qian Wang (Institute of Microbiology, Chinese Academy of Sciences) for technical support in analytical ultracentrifugation.

AUTHOR CONTRIBUTIONS

J.F., T.Z., Y.Z., and Y.L. designed the experiments; J.F. performed the experiments; J.F., T.Z., Y.Z., and Y.L. analyzed the data; Y.L. and T.Z. supervised the study; Y.L., T.Z., and J.F. wrote and revised the manuscript. All authors read and approved the final manuscript.

DECLARATION OF INTERESTS

The authors declare that they have no conflict of interest.

Received: February 3, 2023
Revised: May 11, 2023
Accepted: November 20, 2023
Published: November 22, 2023

REFERENCES

1. Govorunova, E.G., Sineshchekov, O.A., Li, H., and Spudich, J.L. (2017). Microbial rhodopsins: diversity, mechanisms, and optogenetic applications. Annu. Rev. Biochem. *86*, 845–872.
2. Philosof, A., and Béjà, O. (2013). Bacterial, archaeal and viral-like rhodopsins from the Red Sea. Environ. Microbiol. Rep. *5*, 475–482.
3. Gómez-Consarnau, L., Raven, J.A., Levine, N.M., Cutter, L.S., Wang, D., Seegers, B., Arístegui, J., Fuhrman, J.A., Gasol, J.M., and Sañudo-Wilhelmy, S.A. (2019). Microbial rhodopsins are major contributors to the solar energy captured in the sea. Sci. Adv. *5*, eaaw8855.
4. Kouyama, T., and Murakami, M. (2010). Structural divergence and functional versatility of the rhodopsin superfamily. Photochem. Photobiol. Sci. *9*, 1458–1465.
5. Spudich, J.L., Yang, C.S., Jung, K.H., and Spudich, E.N. (2000). Retinylidene proteins: structures and functions from archaea to humans. Annu. Rev. Cell Dev. Biol. *16*, 365–392.
6. Béjà, O., Aravind, L., Koonin, E.V., Suzuki, M.T., Hadd, A., Nguyen, L.P., Jovanovich, S.B., Gates, C.M., Feldman, R.A., Spudich, J.L., et al. (2000). Bacterial rhodopsin: evidence for a new type of phototrophy in the sea. Science *289*, 1902–1906.
7. Doi, S., Mori, A., Tsukamoto, T., Reissig, L., Ihara, K., and Sudo, Y. (2015). Structural and functional roles of the N- and C-terminal extended modules in channelrhodopsin-1. Photochem. Photobiol. Sci. *14*, 1628–1636.
8. Engelhard, C., Chizhov, I., Siebert, F., and Engelhard, M. (2018). Microbial halorhodopsins: light-driven chloride pumps. Chem. Rev. *118*, 10629–10645.
9. Spudich, J.L., and Bogomolni, R.A. (1992). Sensory rhodopsin I: receptor activation and signal relay. J. Bioenerg. Biomembr. *24*, 193–200.
10. Spudich, J.L., and Luecke, H. (2002). Sensory rhodopsin II: functional insights from structure. Curr. Opin. Struct. Biol. *12*, 540–546.
11. Yamauchi, Y., Konno, M., Yamada, D., Yura, K., Inoue, K., Béjà, O., and Kandori, H. (2019). Engineered functional recovery of microbial rhodopsin without retinal-binding lysine. Photochem. Photobiol. *95*, 1116–1121.
12. Olson, D.K., Yoshizawa, S., Boeuf, D., Iwasaki, W., and DeLong, E.F. (2018). Proteorhodopsin variability and distribution in the North Pacific Subtropical Gyre. ISME J. *12*, 1047–1060.
13. Becker, E.A., Yao, A.I., Seitzer, P.M., Kind, T., Wang, T., Eigenheer, R., Shao, K.S.Y., Yarov-Yarovoy, V., and Facciotti, M.T. (2016). A large and phylogenetically diverse class of type 1 opsins lacking a canonical retinal binding site. PLoS One *11*, e0156543.
14. Bieszke, J.A., Li, L., and Borkovich, K.A. (2007). The fungal opsin gene *nop-1* is negatively-regulated by a component of the blue light sensing pathway and influences conidiation-specific gene expression in *Neurospora crassa*. Curr. Genet. *52*, 149–157.
15. Song, Y., Cartron, M.L., Jackson, P.J., Davison, P.A., Dickman, M.J., Zhu, D., Huang, W.E., and Hunter, C.N. (2019). Proteorhodopsin overproduction enhances the long-term viability of *Escherichia coli*. Appl. Environ. Microbiol. *86*, e02087-19.
16. Feng, S., Powell, S.M., Wilson, R., and Bowman, J.P. (2013). Light-stimulated growth of proteorhodopsin-bearing sea-ice psychrophile *Psychroflexus torquis* is salinity dependent. ISME J. *7*, 2206–2213.
17. Kim, J.Y.H., Jo, B.H., Jo, Y., and Cha, H.J. (2012). Improved production of biohydrogen in light-powered *Escherichia coli* by co-expression of proteorhodopsin and heterologous hydrogenase. Microb. Cell Factories *11*, 2.
18. Kuniyoshi, T.M., Balan, A., Schenberg, A.C.G., Severino, D., and Hallenbeck, P.C. (2015). Heterologous expression of proteorhodopsin enhances H_2 production in *Escherichia coli* when endogenous Hyd-4 is overexpressed. J. Biotechnol. *206*, 52–57.
19. Pushkarev, A., Inoue, K., Larom, S., Flores-Uribe, J., Singh, M., Konno, M., Tomida, S., Ito, S., Nakamura, R., Tsunoda, S.P., et al. (2018). A distinct abundant group of microbial rhodopsins discovered using functional metagenomics. Nature *558*, 595–599.
20. Wang, Y., Li, Y., Xu, T., Shi, Z., and Wu, Q. (2015). Experimental evidence for growth advantage and metabolic shift stimulated by photophosphorylation of proteorhodopsin expressed in *Escherichia coli* at anaerobic condition. Biotechnol. Bioeng. *112*, 947–956.
21. Chen, Q., Arents, J., Schuurmans, J.M., Ganapathy, S., de Grip, W.J., Cheregi, O., Funk, C., Branco Dos Santos, F., and Hellingwerf, K.J. (2019). Functional expression of *Gloeobacter* rhodopsin in PSI-less *Synechocystis* sp. PCC 6803. Front. Bioeng. Biotechnol. *7*, 67.
22. Giovannoni, S.J., Bibbs, L., Cho, J.C., Stapels, M.D., Desiderio, R., Vergin, K.L., Rappé, M.S., Laney, S., Wilhelm, L.J., Tripp, H.J., et al. (2005). Proteorhodopsin in the ubiquitous marine bacterium SAR11. Nature *438*, 82–85.
23. Riedel, T., Tomasch, J., Buchholz, I., Jacobs, J., Kollenberg, M., Gerdts, G., Wichels, A., Brinkhoff, T., Cypionka, H., and Wagner-Döbler, I. (2010). Constitutive expression of the proteorhodopsin gene by a flavobacterium strain representative of the proteorhodopsin-producing microbial community in the North Sea. Appl. Environ. Microbiol. *76*, 3187–3197.
24. Schwalbach, M.S., Brown, M., and Fuhrman, J.A. (2005). Impact of light on marine bacterioplankton community structure. Aquat. Microb. Ecol. *39*, 235–245.
25. Kirchman, D.L., and Hanson, T.E. (2013). Bioenergetics of photoheterotrophic bacteria in the oceans. Environ. Microbiol. Rep. *5*, 188–199.
26. Moore, J.P., Li, H., Engmann, M.L., Bischof, K.M., Kunka, K.S., Harris, M.E., Tancredi, A.C., Ditmars, F.S., Basting, P.J., George, N.S., et al. (2019). Inverted regulation of multidrug efflux pumps, acid resistance, and porins in benzoate-evolved *Escherichia coli* K-12. Appl. Environ. Microbiol. *85*, e00966-19.
27. Akram, N., Palovaara, J., Forsberg, J., Lindh, M.V., Milton, D.L., Luo, H., González, J.M., and Pinhassi, J. (2013). Regulation of proteorhodopsin gene expression by nutrient limitation in the marine bacterium *Vibrio* sp. Environ. Microbiol. *15*, 1400–1415.
28. Gómez-Consarnau, L., Akram, N., Lindell, K., Pedersen, A., Neutze, R., Milton, D.L., González, J.M., and Pinhassi, J. (2010). Proteorhodopsin phototrophy promotes survival of marine bacteria during starvation. PLoS Biol. *8*, e1000358.
29. Gómez-Consarnau, L., González, J.M., Coll-Lladó, M., Gourdon, P., Pascher, T., Neutze, R., Pedrós-Alió, C., and Pinhassi, J. (2007). Light stimulates growth of proteorhodopsin-containing marine Flavobacteria. Nature *445*, 210–213.
30. Terashima, M., Ohashi, K., Takasuka, T.E., Kojima, H., and Fukui, M. (2019). Antarctic heterotrophic bacterium *Hymenobacter nivis* $P3^T$ displays light-enhanced growth and expresses putative photoactive proteins. Environ. Microbiol. Rep. *11*, 227–235.
31. Choi, A.R., Shi, L., Brown, L.S., and Jung, K.H. (2014). Cyanobacterial light-driven proton pump, *Gloeobacter* rhodopsin: complementarity between rhodopsin-based energy production and photosynthesis. PLoS One *9*, e110643.
32. Krogh, A., Larsson, B., von Heijne, G., and Sonnhammer, E.L. (2001). Predicting transmembrane protein topology with a hidden Markov model: application to complete genomes. J. Mol. Biol. *305*, 567–580.
33. Darwin, A.J. (2005). The phage-shock-protein response. Mol. Microbiol. *57*, 621–628.
34. Flores-Kim, J., and Darwin, A.J. (2016). The phage shock protein response. Annu. Rev. Microbiol. *70*, 83–101.
35. Phadtare, S., Alsina, J., and Inouye, M. (1999). Cold-shock response and cold-shock proteins. Curr. Opin. Microbiol. *2*, 175–180.
36. Wolska, K.I. (1994). The cold shock response in microorganisms. Acta Biochim. Pol. *41*, 367–374.
37. Smirnova, G.V., Muzyka, N.G., Ushakov, V.Y., Tyulenev, A.V., and Oktyabrsky, O.N. (2015). Extracellular superoxide provokes glutathione efflux from *Escherichia coli* cells. Res. Microbiol. *166*, 609–617.
38. Sýkora, J., Bourová, L., Hof, M., and Svoboda, P. (2009). The effect of detergents on trimeric G-protein activity in isolated plasma membranes from rat brain cortex: correlation with studies of DPH and Laurdan fluorescence. Biochim. Biophys. Acta *1788*, 324–332.
39. He, T.F., Wang, L.H., Niu, D.B., Wen, Q.H., and Zeng, X.A. (2019). Cinnamaldehyde inhibit *Escherichia coli* associated with membrane disruption and oxidative damage. Arch. Microbiol. *201*, 451–458.

40. Ernst, O.P., and Menon, A.K. (2015). Phospholipid scrambling by rhodopsin. Photochem. Photobiol. Sci. *14*, 1922–1931.
41. Menon, I., Huber, T., Sanyal, S., Banerjee, S., Barré, P., Canis, S., Warren, J.D., Hwa, J., Sakmar, T.P., and Menon, A.K. (2011). Opsin is a phospholipid flippase. Curr. Biol. *21*, 149–153.
42. Verchère, A., Ou, W.L., Ploier, B., Morizumi, T., Goren, M.A., Bütikofer, P., Ernst, O.P., Khelashvili, G., and Menon, A.K. (2017). Light-independent phospholipid scramblase activity of bacteriorhodopsin from *Halobacterium salinarum*. Sci. Rep. *7*, 9522.
43. Wu, N., Cernysiov, V., Davidson, D., Song, H., Tang, J., Luo, S., Lu, Y., Qian, J., Gyurova, I.E., Waggoner, S.N., et al. (2020). Critical role of lipid scramblase TMEM16F in phosphatidylserine exposure and repair of plasma membrane after pore formation. Cell Rep. *30*, 1129–1140.e5.
44. Rigaud, J.L., and Lévy, D. (2003). Reconstitution of membrane proteins into liposomes. Methods Enzymol. *372*, 65–86.
45. Shihoya, W., Inoue, K., Singh, M., Konno, M., Hososhima, S., Yamashita, K., Ikeda, K., Higuchi, A., Izume, T., Okazaki, S., et al. (2019). Crystal structure of heliorhodopsin. Nature *574*, 132–136.
46. Jumper, J., Evans, R., Pritzel, A., Green, T., Figurnov, M., Ronneberger, O., Tunyasuvunakool, K., Bates, R., Žídek, A., Potapenko, A., et al. (2021). Highly accurate protein structure prediction with AlphaFold. Nature *596*, 583–589.
47. Bratanov, D., Balandin, T., Round, E., Shevchenko, V., Gushchin, I., Polovinkin, V., Borshchevskiy, V., and Gordeliy, V. (2015). An approach to heterologous expression of membrane proteins. The case of bacteriorhodopsin. PLoS One *10*, e0128390.
48. Feuda, R., Menon, A.K., and Göpfert, M.C. (2022). Rethinking opsins. Mol. Biol. Evol. *39*, msac033.
49. Bonnet, M., Rafi, M.M., Chikindas, M.L., and Montville, T.J. (2006). Bioenergetic mechanism for nisin resistance, induced by the acid tolerance response of *Listeria monocytogenes*. Appl. Environ. Microbiol. *72*, 2556–2563.
50. Charbon, G., Campion, C., Chan, S.H.J., Bjørn, L., Weimann, A., da Silva, L.C.N., Jensen, P.R., and Løbner-Olesen, A. (2017). Re-wiring of energy metabolism promotes viability during hyperreplication stress in *E. coli*. PLoS Genet. *13*, e1006590.
51. Farha, M.A., Verschoor, C.P., Bowdish, D., and Brown, E.D. (2013). Collapsing the proton motive force to identify synergistic combinations against *Staphylococcus aureus*. Chem. Biol. *20*, 1168–1178.
52. Glasser, N.R., Kern, S.E., and Newman, D.K. (2014). Phenazine redox cycling enhances anaerobic survival in *Pseudomonas aeruginosa* by facilitating generation of ATP and a proton-motive force. Mol. Microbiol. *92*, 399–412.
53. Goren, M.A., Morizumi, T., Menon, I., Joseph, J.S., Dittman, J.S., Cherezov, V., Stevens, R.C., Ernst, O.P., and Menon, A.K. (2014). Constitutive phospholipid scramblase activity of a G protein-coupled receptor. Nat. Commun. *5*, 5115.
54. Malvezzi, M., Andra, K.K., Pandey, K., Lee, B.C., Falzone, M.E., Brown, A., Iqbal, R., Menon, A.K., and Accardi, A. (2018). Out-of-the-groove transport of lipids by TMEM16 and GPCR scramblases. Proc. Natl. Acad. Sci. USA *115*, E7033–E7042.
55. Suzuki, J., Umeda, M., Sims, P.J., and Nagata, S. (2010). Calcium-dependent phospholipid scrambling by TMEM16F. Nature *468*, 834–838.
56. Brunner, J.D., Schenck, S., and Dutzler, R. (2016). Structural basis for phospholipid scrambling in the TMEM16 family. Curr. Opin. Struct. Biol. *39*, 61–70.
57. Coleman, J.A., Quazi, F., and Molday, R.S. (2013). Mammalian P4-ATPases and ABC transporters and their role in phospholipid transport. Biochim. Biophys. Acta *1831*, 555–574.
58. López-Marqués, R.L., Poulsen, L.R., Bailly, A., Geisler, M., Pomorski, T.G., and Palmgren, M.G. (2015). Structure and mechanism of ATP-dependent phospholipid transporters. Biochim. Biophys. Acta *1850*, 461–475.
59. Coleman, J.A., Vestergaard, A.L., Molday, R.S., Vilsen, B., and Andersen, J.P. (2012). Critical role of a transmembrane lysine in aminophospholipid transport by mammalian photoreceptor P4-ATPase ATP8A2. Proc. Natl. Acad. Sci. USA *109*, 1449–1454.
60. Marx, U., Lassmann, G., Holzhütter, H.G., Wüstner, D., Müller, P., Höhlig, A., Kubelt, J., and Herrmann, A. (2000). Rapid flip-flop of phospholipids in endoplasmic reticulum membranes studied by a stopped-flow approach. Biophys. J. *78*, 2628–2640.
61. Pomorski, T.G., and Menon, A.K. (2016). Lipid somersaults: uncovering the mechanisms of protein-mediated lipid flipping. Prog. Lipid Res. *64*, 69–84.
62. Hussain, S., Kinnebrew, M., Schonenbach, N.S., Aye, E., and Han, S. (2015). Functional consequences of the oligomeric assembly of proteorhodopsin. J. Mol. Biol. *427*, 1278–1290.
63. Idso, M.N., Baxter, N.R., Narayanan, S., Chang, E., Fisher, J., Chmelka, B.F., and Han, S. (2019). Proteorhodopsin function is primarily mediated by oligomerization in different micellar surfactant solutions. J. Phys. Chem. B *123*, 4180–4192.
64. Maciejko, J., Mehler, M., Kaur, J., Lieblein, T., Morgner, N., Ouari, O., Tordo, P., Becker-Baldus, J., and Glaubitz, C. (2015). Visualizing specific cross-protomer interactions in the homo-oligomeric membrane protein proteorhodopsin by dynamic-nuclear-polarization-enhanced solid-state NMR. J. Am. Chem. Soc. *137*, 9032–9043.
65. Finkel, O.M., Béjà, O., and Belkin, S. (2013). Global abundance of microbial rhodopsins. ISME J. *7*, 448–451.
66. Lyu, X., Shen, C., Fu, Y., Xie, J., Jiang, D., Li, G., and Cheng, J. (2015). The microbial opsin homolog sop1 is involved in *Sclerotinia sclerotiorum* development and environmental stress response. Front. Microbiol. *6*, 1504.
67. Schuck, P. (2000). Size-distribution analysis of macromolecules by sedimentation velocity ultracentrifugation and lamm equation modeling. Biophys. J. *78*, 1606–1619.
68. Kumar, S., Stecher, G., and Tamura, K. (2016). MEGA7: molecular evolutionary genetics analysis version 7.0 for bigger datasets. Mol. Biol. Evol. *33*, 1870–1874.
69. Baba, T., Ara, T., Hasegawa, M., Takai, Y., Okumura, Y., Baba, M., Datsenko, K.A., Tomita, M., Wanner, B.L., and Mori, H. (2006). Construction of *Escherichia coli* K-12 in-frame, single-gene knockout mutants: the Keio collection. Mol. Syst. Biol. *2*.

STAR★METHODS

KEY RESOURCES TABLE

REAGENT or RESOURCE	SOURCE	IDENTIFIER
Antibodies		
6× His tag antibody	GeneTex	Cat#GTX628914; RRID: AB_2750602
Goat Anti-Mouse IgG antibody (HRP)	GeneTex	Cat#GTX213111-01; RRID: AB_10618076
Bacterial and virus strains		
E. coli BW25113	Lab stock	N/A
E. coli C43(DE3)	Beyotime	Cat#D1023
Chemicals, peptides, and recombinant proteins		
All *trans*-retinal	Sigma-Aldrich	CAS#116-31-4
Carbonyl cyanide 3-chlorophenylhydrazone	Sigma-Aldrich	CAS#555-60-2
Bis-(1,3-dibutylbarbituric acid)trimethine oxonol	Dojindo	CAS#70363-83-6
1,6-diphenyl-1,3,5-hexatriene	Sigma-Aldrich	CAS#1720-32-7
n-dodecyl-β-*d*-maltoside	Aladdin	CAS#69227-93-6
1-palmitoyl-2-oleoyl-*glycero*-3-phosphocholine	Avanti	CAS#26853-31-6
1,2-dioleoyl-*sn*-glycero-3-phospho-*l*-serine	Avanti	CAS#90693-88-2
1,2-dipalmitoyl-*sn*-glycero-3-phosphoethanolamine-*N*-(7-nitro-2,3-benzoxadiazol-4-yl)	Avanti	CAS#384823-46-5
Critical commercial assays		
Enhanced ATP Assay Kit	Beyotime	Cat#S0027
Deposited data		
Psychroflexus torquis ATCC 700755, complete genome	National Center for Biotechnology Information	GenBank Accession Number CP003879.1
Bacteriorhodopsin, structure	RCSB Protein DataBank	PDB ID 4MD2
Oligonucleotides		
Primers	See Table S2	N/A
Software and algorithms		
NIS-Elements Viewer	Nikon	https://www.microscope.healthcare.nikon.com
FlowJo	Becton Dickinson	https://www.flowjo.com
SEDFIT	Schuck et al.[67]	https://sedfitsedphat.github.io
MEGA	Kumar et al.[68]	https://megasoftware.net
AlphaFold	Jumper et al.[46]	https://github.com/deepmind/alphafold

RESOURCE AVAILABILITY

Lead contact

Further information and requests for resources and reagents should be directed to and will be fulfilled by the lead contact, Yin Li (yli@im.ac.cn).

Materials availability

This study did not generate new unique reagents.

Data and code availability

The datasets used and/or analyzed during the current study are available from the corresponding authors on reasonable request.

This paper does not report original code.
Any additional information required to reanalyze the data reported in this paper is available from the lead contact upon request.

EXPERIMENTAL MODEL AND STUDY PARTICIPANT DETAILS

Bacterial strains

The *E. coli* strain BW25113[69] was used in this study. The medium and cultivation condition were described in method details.

METHOD DETAILS

Plasmids, bacterial strains and growth conditions

For the expression of ptqPR (GenBank: AFU67218.1), a codon-optimized gene was synthesized by Shanghai Generay Biotech (Shanghai, China). The fragment was cloned into the pED31 expression vector, and the resulted construct pED31-ptqPR was transformed into *E. coli* BW25113, designated as BW/ptqPR^{+}. The BW25113 strain harboring an empty pED31 plasmid was designated as BW/ptqPR^{-}. For site-directed mutagenesis of the *ptqPR* gene, the plasmid pED31-ptqPR was subjected to mismatch PCR using overlapping primers containing the corresponding mutation sites. The PCR products were transformed into *E. coli* DH5α to generate corresponding mutation ptqPR expression vectors, which were subsequently transformed into *E. coli* BW25113.

E. coli was routinely cultured in LB medium at 37°C, 220 rpm and induced with 0.25 mM IPTG; 50 μg/mL kanamycin was added when necessary. For testing the growth and physiological properties of *E. coli*, M9 medium with 10 g/L glucose was used. The M9 medium contains Na_2HPO_4 17.1 g/L, KH_2PO_4 3 g/L, NaCl 0.5 g/L, NH_4Cl 1 g/L, $MgSO_4$ 2 mM, $CaCl_2$ 0.1 mM. Cells were inoculated into M9 medium (containing 50 μg/mL kanamycin and 0.25 mM IPTG) to an initial cell density of OD_{600} of 0.1 from overnight culture in LB medium and cultivated at 37°C in a static incubator. For all cultures, illumination (100 μE $m^{-2}\cdot s^{-1}$) and retinal (10 μM) were used when necessary.

ATP measurement

The intracellular ATP levels were measured by using an Enhanced ATP Assay Kit (Beyotime Biotechnology, Shanghai, China) following the manufacturer's instruction. Cells grown in different conditions were collected by centrifugation (4°C, 12,000×*g*, 2 min) and resuspended in 20 mM Tris-HCl buffer (pH 8.0). The suspended cells were lysed by sonication on ice for 5 min (3 s pulses, 3 s pauses, 25% amplitude) and centrifuged (4°C, 12,000×*g*, 5 min). The resulting supernatant was dispensed into the detection reagent and then the luminescence intensity was measured by microplate reader (Infinite M200 Pro, Tecan). The concentration of ATP was calculated according to the standard curve and expressed as nmol ATP per dry cell weight.

Light-driven proton-pumping assay

Cells were cultivated and induced in LB medium overnight. The pellets were washed twice with 150 mM NaCl solution and resuspended in the same solution. The cell suspension was firstly placed in darkness for 5 min and then illuminated by a LED light source with an intensity of 150 μE $m^{-2}\cdot s^{-1}$, then a 5 min/5 min light-dark cycle was applied. pH changes were measured by recording solution pH every minute with a pH meter.

Transcriptome analysis

mRNA sequencing and raw data analysis were performed by GENEWIZ (Suzhou, China). Samples were collected from cells grown in M9 medium for 12 h. Total RNA of each sample was extracted using RNeasy Mini Kit (Qiagen), then quantified and qualified by Agilent 2100 Bioanalyzer (Agilent Technologies), NanoDrop (Thermo Fisher Scientific) and 1% agarose gel. The next-generation sequencing libraries were constructed and then multiplexed and loaded on an Illumina HiSeq according to the manufacturer's instruction.

Determination of membrane potential

An anionic lipophilic potential sensitive dye bis-(1,3-dibutylbarbituric acid)trimethine oxonol [$DiBAC_4(3)$] (Dojindo) was used for the measurement of membrane potential.[37] Cultures grown in M9 medium overnight were collected and incubated with adding 10 μg/mL $DiBAC_4(3)$ at 37°C for 10 min. Then the fluorescent intensity was measured by a microplate reader (Infinite M200 Pro, Tecan) with an excitation wavelength of 488 nm and an emission wavelength of 540 nm.

Determination of membrane fluidity

A fluorescent probe 1,6-diphenyl-1,3,5-hexatriene (DPH) was used for the measurement of membrane fluidity through the calculation of membrane polarization.[38] Cultures grown in M9 medium overnight were collected and incubated with adding 1 μM at 37°C for 30 min. Then the polarized fluorescent intensity was measured by a fluorescence spectrometer (F-7000, Hitachi) with an excitation wavelength of 360 nm and an emission wavelength of 450 nm. The polarized fluorescence was calculated as follows: $P=(I_{VV}-GI_{VH})/(I_{VV}+GI_{VH})$, where I_{VV} is the fluorescent intensity measured with both excitation and emission polarized vertically, and I_{VH} is the fluorescent intensity measured with vertically polarized excitation and horizontally polarized emission. The correlation factor G was calculated as: $G = I_{HV}/I_{HH}$, where I_{HV} is the fluorescent intensity measured with horizontally polarized excitation and vertically polarized emission, and I_{HH} is the fluorescent intensity measured with both excitation and emission polarized horizontally.

Determination of membrane permeability

The membrane permeability was determined by measuring the electrolyte leakage[39] using a conductivity meter (HI8633, HANNA). Cells were cultivated and induced in LB medium overnight and centrifuged (4,500×*g*, 5 min). The pellets were washed three times with 5% glucose and resuspended in the same solution. Then the measurement of conductivity was performed at different points in time. The relative electric conductivity was calculated as follows: $E=(E_2-E_1)/E_0$, where E_1 is the conductivity of 5% glucose and E_2 is the conductivity of the suspension incubated for different times, and E_0 is the conductivity of the suspension finally treated in boiling water for 15 min.

Protein purification

The *ptqPR* gene was subcloned into a pET-30a vector with C-terminal 6×His-tag and the construct was transformed into *E. coli* C43(DE3) strain for protein expression. Transformed cells were cultivated in LB medium at 37°C to an OD_{600} of 0.6, and protein expression was induced by 0.25 mM IPTG at 18°C for 18 h. Cells were harvested by centrifugation (4°C, 6,000×*g*, 5 min) and resuspended in Buffer A (50 mM Tris-HCl, 150 mM NaCl, pH 8.0), then lysed by sonication on ice. The membrane fraction was collected by ultracentrifugation (4°C, 120,000×*g*, 2 h) and the pellet was solubilized with Buffer B (50 mM Tris-HCl, 150 mM NaCl, 1.5% *n*-dodecyl-β-D-maltoside (DDM), pH 8.0) by rotating at 4°C for 3 h. The insoluble material was removed by ultracentrifugation (4°C, 120,000×*g*, 30 min) and the soluble fraction was incubated with Ni-NTA Agarose (Qiagen) at 4°C for 3 h. After loading, the sample was washed with Buffer C (50 mM Tris-HCl, 300 mM NaCl, 50 mM imidazole, 0.1% DDM, pH 8.0). Then, protein was eluted with Buffer D (50 mM Tris-HCl, 300 mM NaCl, 500 mM imidazole, 0.1% DDM, pH 8.0). The purified protein was concentrated and finally solubilized in Buffer E (50 mM Tris-HCl, 150 mM NaCl, 0.1% DDM, pH 8.0) by an Amicon Ultra-0.5 centrifugal filter (Millipore).

Preparation of small unilamellar vesicles and proteoliposomes

Small unilamellar vesicles (SUVs) were prepared from 1-palmitoyl-2-oleoyl-*glycero*-3-phosphocholine (POPC), 1,2-dioleoyl-*sn*-glycero-3-phospho-L-serine (DOPS) and 1,2-dipalmitoyl-*sn*-glycero-3-phosphoethanolamine-*N*-(7-nitro-2,3-benzoxadiazol-4-yl) (NBD-PE) at a molar ratio of 84:15:1. Lipids were mixed in chloroform and dried to obtain a thin film, then placed under vacuum for 3 h to remove residual organic solvent. The resulting lipid film was resuspended in Buffer A to a total lipid concentration of 10 mM. The lipid suspension was repeatedly frozen in liquid nitrogen and thawed in warm water for ten cycles. The lipid solution was extruded using a mini-extruder (Avanti) with 100-nm polycarbonate membrane filter (Whatman) by repeatedly passing through the membrane filter for 11 times.

Proteoliposomes were prepared by reconstitution of proteins into SUVs using a detergent-mediated method. SUVs were diluted to a total lipid concentration of 2 mM, and DDM was added to a final concentration of 0.11% according to the detergent-saturated concentration of liposomes. Then proteins were added to the mixture and incubated at 4°C for 1 h. For complete detergent removal, four sequential additions were made every hour at 4°C with a fifth addition for overnight incubation using Bio-Beads SM-2 (Bio-Rad). Bio-Beads SM-2 were gradually added at increasing amounts each time.

Scramblase activity assay

The NBD-labeled proteoliposomes containing ptqPR were used for *in vitro* scramblase activity assay. The reconstitution of proteoliposome was performed as described above. Purified ptqPR protein was added at a protein/phospholipid molar ratio of 1:1,000.

The NBD fluorescence was monitored by a microplate reader (Infinite M200 Pro, Tecan) with an excitation wavelength of 470 nm and an emission wavelength of 530 nm. Sodium dithionite was added to a final concentration of 20 mM and 1% Triton X-100 was added after 15 min. The NBD-PE scrambled from inside membrane to outside membrane was calculated as follows: $N=(F_0-F_1)/(F_0-F_2)-0.5$, where F_0 is the initial fluorescent intensity before adding sodium dithionite, F_1 is the fluorescent intensity 15 min after adding sodium dithionite, and F_2 is the fluorescent intensity 15 min after adding Triton X-100.

QUANTIFICATION AND STATISTICAL ANALYSIS

All experiments were performed in triplicate and all data were shown as mean ± standard deviation. Student's *t* test was applied to analyze the comparison among different groups. p values < 0.05 were considered statistically significant.